Physics – Uspekhi **59** (7) 702 – 712 (2016)

CONFERENCES AND SYMPOSIA

PACS numbers: **04.70.–s**, 97.60.Lf, 98.62.Js

Observing stellar-mass and supermassive black holes

A M Cherepashchuk

DOI: 10.3367/UFNe.2015.12.037736

Contents

Abstract. During the last 50 years, great progress has been made in observing stellar-mass black holes (BHs) in binary systems and supermassive BHs in galactic nuclei. In 1964, Zeldovich and Salpeter showed that in the case of nonspherical accretion of matter onto a BH, huge energy releases occur. The theory of disk accretion of matter onto BHs was developed in 1972–1973 by Shakura and Sunyaev, Pringle and Rees, and Novikov and Thorne. Up to now, 100 years after the creation of Albert Einstein's General Theory of Relativity, which predicts the existence of BHs, the masses of tens of stellar-mass BHs ($M_{BH} = (4-35)\,M_\odot$) and many hundreds of supermassive BHs ($M_{BH} = (10^6-10^{10})\,M_\odot$) have been determined. A new field of astrophysics, so-called BH demography, is developing. The recent discovery of gravitational waves from BH mergers in binary systems opens a new era in BH studies.

Keywords: black holes, binary stars, galactic nuclei, event horizon, accretion

1. Introduction

Astronomical studies of black holes (BHs) in the Universe have been carried out during the last 50 years. Observational studies of BHs were initiated by the pioneering papers by Zel'dovich [1] and Salpeter [2], which showed that huge energy is released during nonspherical accretion of matter onto a BH. The theory of disk accretion of matter onto BHs was developed by Shakura and Sunyaev [3], Pringle and Rees [4], and Novikov and Thorne [5]. In 2015, we celebrated 100 years of Albert Einstein's formulation of General Relativity (GR), which predicts the existence of BHs — compact objects (more precisely, regions of space–time) with a gravitational field so strong that no signal, including light, can escape from them to infinity.

A M Cherepashchuk. Lomonosov Moscow State University, Sternberg Astronomical Institute, Universitetskii prosp. 13, 119991 Moscow, Russian Federation

Received 16 February 2016
Uspekhi Fizicheskikh Nauk **186** (7) 778 –789 (2016)
DOI: 10.3367/UFNr.2015.12.037736
Translated by K A Postnov; edited by A M Semikhatov

To date, great progress has been achieved in observations of both stellar-mass BHs in X-ray binary systems ($M_{BH} \approx (4-16)\,M_\odot$) and supermassive BHs (SMBHs) in galactic nuclei ($M_{BH} = (10^6-10^{10})\,M_\odot$).

Since February 11, 2016, a qualitatively new stage in BH studies began, related to the discovery of gravitational waves from coalescing BHs in binary systems [6]. In addition, under way is an advanced ground-based Very Long Baseline Interferometry (VLBI) project at short waves ($\lambda \lesssim 1.3$ mm) of the EHT (Event Horizon Telescope), with an angular resolution of the order of 10^{-5} arcsec [7–10], which is aimed at imaging dark 'shadows' from BHs on accretion disks and relativistic jets in nearby galactic nuclei (the center of our Galaxy, with $M_{BH} \approx 4.3 \times 10^6 M_\odot$, and the center of the galaxy M87, with $M_{BH} \approx 6 \times 10^9 M_\odot$).

There are big hopes to probe the surroundings of SMBHs in galactic nuclei by the Radioastron space radio interferometer and the future short-wave space interferometer Millimetron [11].

According to conservative estimates, the number of stellar-mass BHs in our Galaxy, as derived from the analysis of observational data with account for observational selection effects, is $\sim 10^7$. With the average mass of a BH being $\sim 9-10\,M_\odot$, this makes $\sim 10^8\,M_\odot$, or about 0.1% of the total mass of baryonic matter in the Galaxy. In addition, there is an SMBH with a mass of $4.3 \times 10^6\,M_\odot$ in the center of the Galaxy, which controls the motion of nearby stars in elliptic orbits, observed by modern advanced astronomical means (see, e.g., [12]).

In our review [13], we described the main observational facts on stellar-mass BHs and SMBHs. In this paper, we describe recent observational results in this field.

2. Stellar mass black holes in binary systems

On February 11, 2016, the LIGO (Laser Interferometer Gravitational Wave Observatory) collaboration (which unites scientists from several countries, including Russia), announced the discovery of gravitational waves from a coalescing binary BH. This outstanding discovery was made on September 14, 2015 by two American laser gravitational wave interferometers LIGO separated by ≈ 3000 km [6]. Both antennas registered the gravitational wave signal GW150914 that lasted about two tenths of a second. The

signal has the shape of quasi-sine oscillations with a decreasing period and increasing amplitude with an abrupt decay. The observed gravitational wave signal is well fitted by a theoretical waveform (the 'light curve') calculated in GR [14] from two coalescing BHs in a binary system. The corresponding initial masses of the BHs are $36^{+5}_{-4} M_\odot$ and $29^{+4}_{-4} M_\odot$. The final mass of the BH after coalescence is $62^{+4}_{-4} M_\odot$, with $3.0^{+0.5}_{-0.5} M_\odot$ emitted in the form of gravitational waves. The source is located at a distance of 410^{+160}_{-180} Mpc from Earth (the corresponding redshift is $z = 0.09^{+0.03}_{-0.04}$). The quoted errors are at a 90% confidence level. The authors of remarkable paper [6] conclude that their observations prove the existence of binary systems consisting of stellar-mass BHs. They also stress that they for the first time managed to directly detect gravitational waves and to observe the process of coalescence of BHs.

It is interesting to note that the first detection of gravitational waves from coalescing BHs and not from neutron stars was predicted in papers [15, 16].

It is important to stress that paper [6] opens a new way of searching for stellar-mass BHs in the Universe and offers the unique possibility of probing geometrodynamics — the nonlinear dynamics of curved spacetime [14].

We now discuss the latest data on stellar-mass BHs in X-ray binary systems.

Of the 26 known X-ray binaries with BHs, 17 are low-mass X-ray binaries (LMXBs), in which the optical companion is a K–M–A low-mass star (with the typical mass $M_v = (0.3-2)\, M_\odot$). Nine systems are quasi-stationary high-mass X-ray binaries (HMXBs) with massive optical early-type O, B, WR companions (with typical masses $M_v = (5-70)\, M_\odot$). The parameters of X-ray binaries with BHs are presented in [13, 17] and in monograph [18], where the main features of these systems are described in detail.

The evolutionary paths of BH LMXBs and BH HMXBs are significantly different [19]. LMXBs evolve through the common envelope stage. In this case, a massive star ($M > 25\, M_\odot$), the BH progenitor, in the course of evolutionary expansion fills its Roche lobe and transfers mass to the low-mass companion star ($M_v \simeq M_\odot$), forming a common envelope. The common envelope forms because the thermal relaxation time of the low-mass ($M_v \simeq M_\odot$) companion star $T_K = GM^2/(RL)$ is much longer than that of the massive primary star, and therefore the matter from the primary star has no time to enter into thermal equilibrium with the low-mass companion, resulting in the common envelope formation.

Due to dynamical friction in the common envelope, the low-mass companion rapidly loses its orbital angular momentum and energy to the envelope, which is then dispersed in the surrounding medium. The orbital period of the binary system is strongly reduced, and the primary star becomes a Wolf–Rayet star with a mass of $\sim 10\, M_\odot$, which, after a supernova type-Ib/c explosion, leaves a stellar-mass BH. If less than half the total mass of the binary system is lost in the supernova explosion, a gravitationally bound close binary system consisting of the BH and the low-mass companion ($M_v \simeq M_\odot$) is left. The further evolution of this system leads to mass transfer from the low-mass star to the BH. An accretion disk forms around the BH, and the system becomes an LMXB.

The HMXBs evolve differently. Because the masses of the components of the initial binary system are comparable, the mass transfer does not result in the common envelope, and an HMXB is formed at the semi-detached stage. The initially more massive star first fills its Roche lobe and transfers up to 50% of its mass through the inner Lagrangian point to the companion and then, after the formation of a Wolf–Rayet star, explodes as a type-Ib/c supernova. Further nuclear evolution of the companion star (whose mass was increased) leads to the Roche lobe overflow and mass transfer to the BH. An accretion disk forms and the system becomes an HMXB. Gravitational wave observations [6] suggest that the subsequent evolution of such an HMXB can lead to the formation of a binary BH system. The system IC10X-1 can be such an HMXB [20].

Apparently, the different evolutionary scenarios of LMXBs and HMXBs are related to the interesting observation that LMXBs and HMXBs have different BH mass distributions (Fig. 1): BHs in LMXBs are concentrated near $\sim 8\, M_\odot$, while BH masses in HMXBs demonstrate a broad uniform distribution.

The first detailed calculations of the evolution of close binaries with a common envelope (see, e.g., [21–24]) showed that it is difficult to expel a massive common envelope into the surrounding medium due to the transfer of the kinetic energy of the orbital motion of the low-mass companion. In the standard evolutionary scenario with a common envelope, a BH LMXB is formed if the mass of the low-mass companion is sufficiently high, at least $M_\odot$. At the same time, observations of BH LMXBs suggest that the mean mass of the optical star in these systems is as low as $0.6\, M_\odot$. In recent paper [25], the mechanisms of LMXB evolution with a common envelope are analyzed in more detail, including the role of

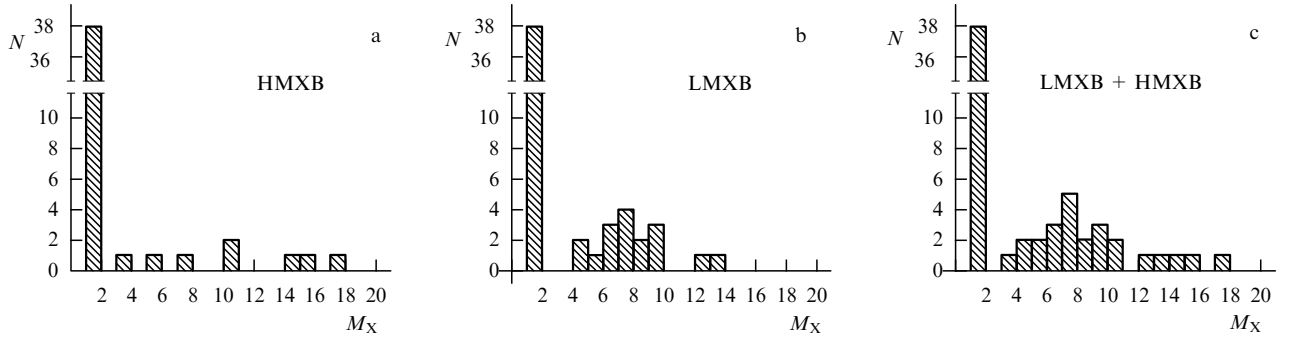

Figure 1. Mass distribution of neutron stars and black holes: (a) in high-mass X-ray binary systems (HMXB) with O-B and WR optical companions; (b) in low-mass X-ray binary systems (LMXB). (c) Total mass distribution of neutron stars and BHs (in high-mass and low-mass binaries). High peaks in the left parts of histograms (a–c) correspond to neutron stars.

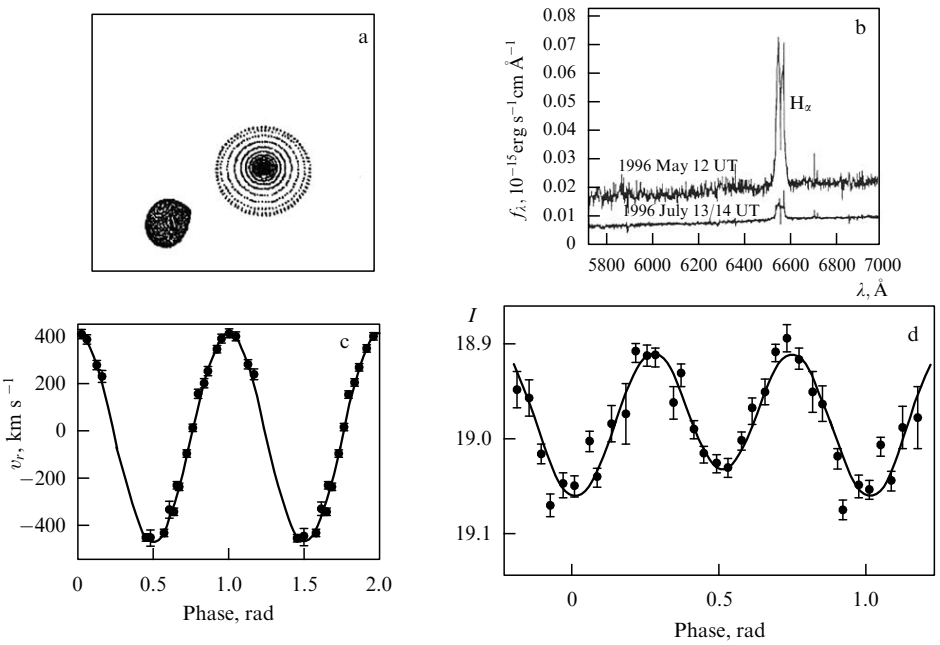

Figure 2. Optical observations that allow determining the BH mass in an X-ray binary system: (a) computer model of the system; (b) spectrum of the X-ray binary at quiescence (between outbursts); (c) radial velocity curve of the optical companion; (d) light curve of the system. The light curve is in units of stellar magnitudes in filter I (the smaller the stellar magnitude is, the higher the radiation intensity).

various model assumptions and parameters, such as supernova explosion mechanisms leading to the BH formation, the binding energy of the common envelope, the efficiency of the orbital kinetic energy transfer to the common envelope, and the initial mass distribution of low-mass companions in LMXBs. Comparing parameters of the calculated BH LMXBs with observations allowed the authors of [25] to constrain the common envelope evolution. In particular, they showed that with the thermal energy of the envelope taken into account, it is possible to form BH LMXBs with acceptable parameters within the standard evolutionary scenario with a common envelope if BHs in these systems were formed from not too massive stars ($M < 28\ M_\odot$) via a 'quiet' collapse of helium or oxygen–carbon cores of these stars without supernova explosion and envelope ejection (failed supernovae [25]). However, observations suggest that at least in some BH LMXBs, the black holes originated from a 'loud' collapse accompanied by a supernova explosion and massive-star envelope ejection, which resulted in enrichment of the low-mass star companion atmosphere by α-elements, which cannot be synthesized in the low-mass star interiors.

For example, the discovery of enhanced absorption lines of α-elements O, Si, and Mg in the spectrum of the optical companion of the BH LMXB GRO1655-40 was reported in [26]. This may suggest the enrichment of the optical star atmosphere by products of the supernova explosion accompanying the BH formation. In addition, this system shows a high peculiar velocity of the barycenter, $v_{\rm pec} = (-144 \pm 19)$ km s^{-1} [27], which can be related to the momentum acquired by the binary system in the supernova explosion. Another BH LMXB, SAXJ1819.3-2525, also demonstrates an enhanced abundance of α-elements in the optical spectrum, suggesting a supernova explosion in the system [28]. The third BH LMXB, XTEJ1118+480, has a very large height above the Galactic plane ($z = 1.7$ kpc [29]) and a high peculiar velocity of the barycenter (~ 145 km s^{-1}) [30], which also may suggest a supernova explosion in this system, resulting in the high barycenter velocity $v_{\rm in} = (217 \pm 18)$ km s^{-1} [30].

Thus, the problem of low optical star masses in BH LMXBs is not finally solved yet. In this connection, it is important to revisit the accuracy of the optical star mass $M_{\rm v}$ determination in LMXBs, which was carried out in our papers [31, 32].

Figure 2b shows the observed optical spectrum of an LMXB in quiescence between outbursts, which includes numerous absorption lines of a late-type optical star. The spectrum shows a powerful double-peak emission line from the accretion disk rotating around a BH. Using Doppler shifts of the absorption lines in the optical spectrum of the low-mass star, it is possible to construct its radial velocity curve — the dependence of the line-of-sight orbital velocity of the optical star on time (Fig. 2c). Measurements of the optical star brightness enable its light curve to be constructed (Fig. 2d). The optical variability of an LMXB in quiescence is mainly due to the elliptical form of the optical star that fills its Roche lobe [33, 34] and the contribution from the accretion disk (see, e.g., [35]). The BH mass is determined by the formula

$$M_{\rm BH} = f_{\rm v}(M)\left(1+\frac{1}{q}\right)^2 \frac{1}{\sin^3 i}\,, \qquad (1)$$

where $q = M_{\rm BH}/M_{\rm v}$ is the mass ratio of the BH and the optical star, i is the orbital inclination angle of the X-ray binary system to the sky plane, and $f_{\rm v}(M)$ is the mass function of the optical star, which is calculated from its radial velocity curve (Fig. 2c):

$$f_{\rm v}(M) = \frac{M_{\rm BH}^3 \sin^3 i}{(M_{\rm BH}+M_{\rm v})^2} = 1.038\times 10^{-7} K_{\rm c}^3 P (1-e^2)^{3/2}\,. \qquad (2)$$

Here, $K_{\rm c}$ is the semi-amplitude of the radial velocity curve of the optical star barycenter (in km s^{-1}), P is the orbital binary period (in days), $M_{\rm BH}$ and $M_{\rm v}$ are the masses of the

components (in solar masses $M_\odot$), and e is the orbital eccentricity derived from the deviation of the radial velocity curve of the system from a pure sine.

Thus, the mass function $f_v(M)$ can be found from the observed radial velocity curve of the optical star. The orbital inclination i is derived from the analysis of the observed light curve (see, e.g., [18]). The mass ratio $q = M_{BH}/M_v$ is determined from the rotational Doppler broadening of absorption lines in the optical star spectrum using the formula (see, e.g., [36])

$$v_{rot} \sin i = 0.468 K_c \frac{1}{q^{1/3}} \left(1 + \frac{1}{q}\right)^{2/3}, \quad (3)$$

where v_{rot} is the equatorial rotational velocity of the star (the value of $v_{rot} \sin i$ can be derived from the observed absorption line profiles).

Formula (3) is obtained from the following considerations. The optical star rotates synchronously with the orbital motion and fills its Roche lobe, whose size depends on the components mass ratio $q = M_{BH}/M_v$. The larger the size of the optical star is (which is equal to the Roche lobe size), the higher the linear rotational velocity at the equator. Hence follows formula (3) for $v_{rot} \sin i$.

Formulas (1)–(3) imply that the accuracy of M_{BH} and M_v determination with given observational errors and a fixed binary inclination i mainly depends on the accuracy of the determination of K_c and q.

We consider systematic determination errors of K_c and q. The value of K_c corresponds to the barycenter of the optical star, which is not a material point but has a pear-like shape with a complex surface temperature distribution caused by gravitational darkening and X-ray illumination effects. Therefore, the observed radial velocity semi-amplitude K_v does not coincide with that of the star barycenter K_c. In [31, 32], K-corrections to the observed radial velocity curves are calculated and tabulated for LMXBs and HMXBs:

$$K_{corr} = \frac{K_v}{K_c},$$

where K_v is the maximum observed radial velocity amplitude of the real star in the Roche model, and K_c is the radial velocity semi-amplitude of the star barycenter. Here, K_v does not necessarily correspond to quadratures at the orbital phase $\phi_{orb} = 0.25$ and 0.75 (Fig. 3). Values of K_{corr} are calculated using special codes [37–39] synthesizing line profiles and radial velocity curves of optical stars in X-ray binary systems.

Figure 4 presents the dependence of the K-corrections on q for HMXBs. It is seen that in HMXBs with small mass ratios q, the K-correction is by about 5% smaller than unity. Therefore, taking the K-correction into account in HMXBs with insignificant X-ray illumination increases M_{BH} by

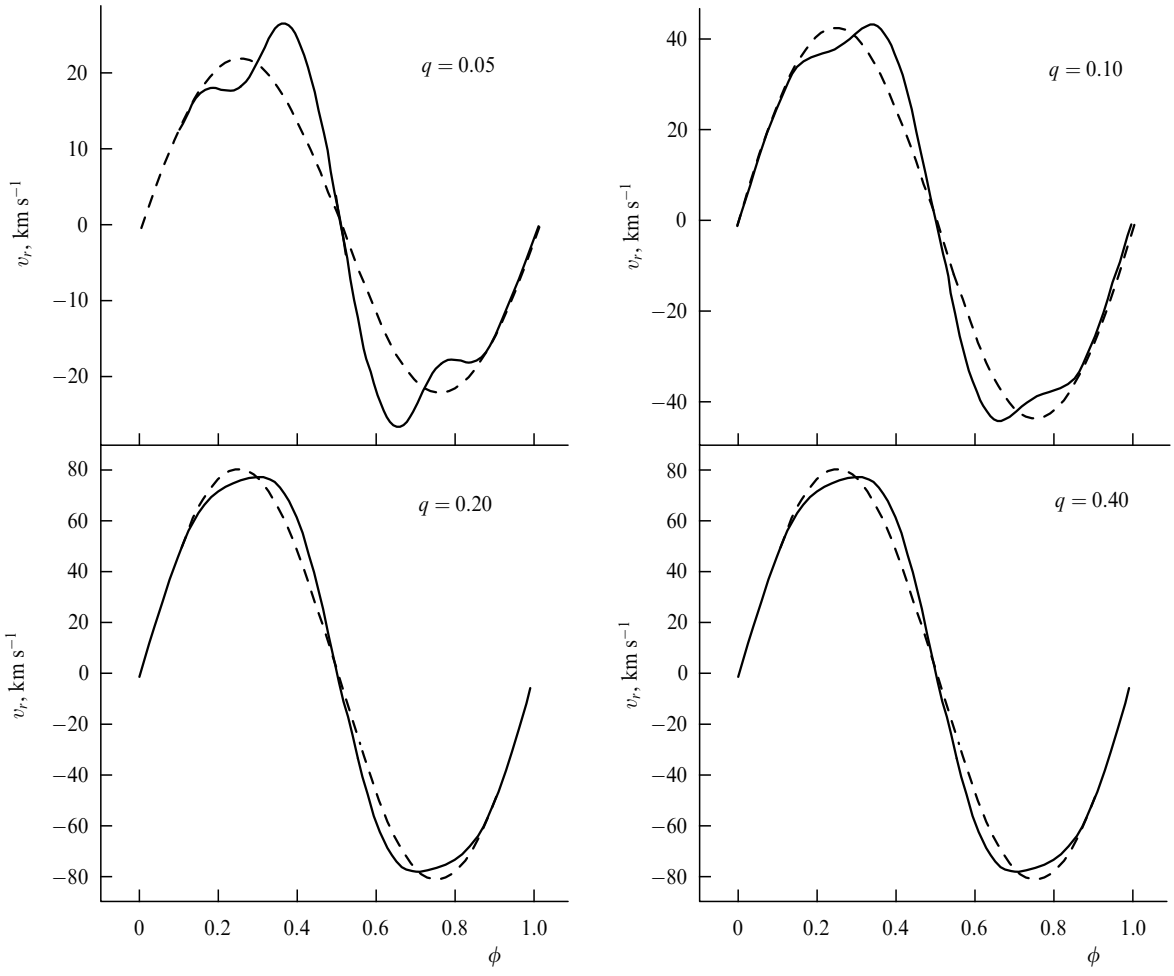

Figure 3. Radial velocity curve of the optical companion of an X-ray binary system as a function of the component mass ratio $q = M_{BH}/M_v$. The solid line shows the radial velocity curve of a tidally distorted star, and the dashed curve shows the radial velocity curve of the star barycenter. The orbit of the binary is circular. (From [31].)

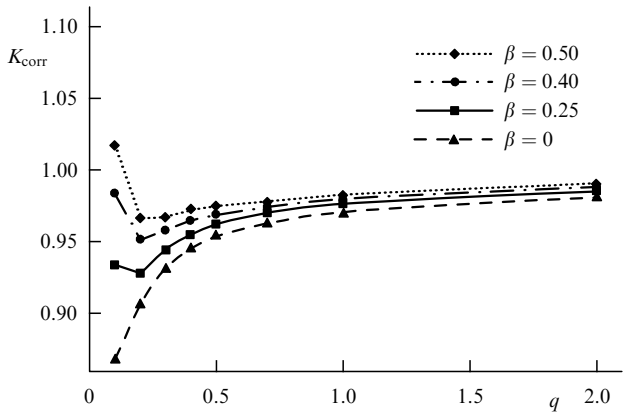

Figure 4. K-corrections for high-mass X-ray binaries as a function of the mass ratio $q = M_{BH}/M_v$ for different gravitational darkening coefficients. For hot O–B stars, $\beta = 0.25$ is usually assumed. (From [31].)

about 10%. In the case of LMXBs, the mass ratio $q = M_{BH}/M_v$ is much larger than unity ($q = 2.3-26$), and for large q, as follows from Eqn (1), the BH mass M_{BH} very weakly depends on q. Therefore, in LMXBs, the K-correction does not significantly affect M_{BH}. For BH LMXBs, is the error in determining q by formula (3) that takes line rotational broadening into account is the most significant. Figure 5 shows the absorption line profiles in the spectrum of a BH LMXB at different orbital phases calculated by our method for a realistic optical star model with account for the tidal–rotational deformation of the star, limb darkening and gravitational darkening effects, as well as X-ray heating from the accreting BH. It is seen that in a realistic model, the absorption line profile significantly changes with the orbital phase. The full width at half maximum (FWHM) of the line changes, and an emission component arises at phases near quadratures due to the X-ray heating. By varying q and comparing the obtained spectra with observations (see Fig. 5), it is possible to determine q in the appropriate model.

The actual situation is more complicated [40]. Low-mass optical stars in LMXBs are very faint ($V \simeq 19-25$); therefore, it is difficult to reliably measure the profiles of individual spectral lines even with big telescopes. To increase accuracy, all line profiles are usually averaged over orbital phases. Moreover, the line profiles are typically broadened by the instrumental spectrograph profile. If the orbital period of a binary system is small (of the order of several hours), a noticeable Doppler broadening caused by the orbital motion of the star occurs during the exposure time, leading to some 'smearing' of the absorption lines. Therefore, to determine q from Eqn (3), a differential method is used. First, the spectrum of a given LMXB is taken, and then the spectrum of a standard nonrotating star is measured by the same spectrograph. Then the lines on the spectrum of the standard star are artificially broadened for different $v_{rot} \sin i$, and the difference between the spectrum of the studied LMXB and the artificially broadened spectrum is minimized. The minimum of this difference (using the χ^2 test) gives the sought value of $v_{rot} \sin i$. As long as one spectrograph is used, this method excludes the effect of the instrumental profile. In addition, because many absorption lines are used, even with a moderate spectral resolution ($R = \lambda/\Delta\lambda \approx 5000$), it is possible to estimate $v_{rot} \sin i$ quite accurately and to calculate q using formula (3).

The artificial broadening of absorption line profiles in the spectrum of a nonrotating standard star uses the classical rotational broadening method (see, e.g., [41]). In this method, the optical star is substituted by a flat circle with the radius equal to the radius of a sphere with the volume of the Roche lobe. The local absorption line profile is assumed to be not broadened and constant at all points of the circle with linear limb darkening. This enables a simple convolution-like equation to be applied to calculate the Doppler broadening of many absorption lines.

In fact, the star has a complex volume structure, a pear-like shape with a complex surface temperature distribution, leading to a strong dependence of the line profile on the

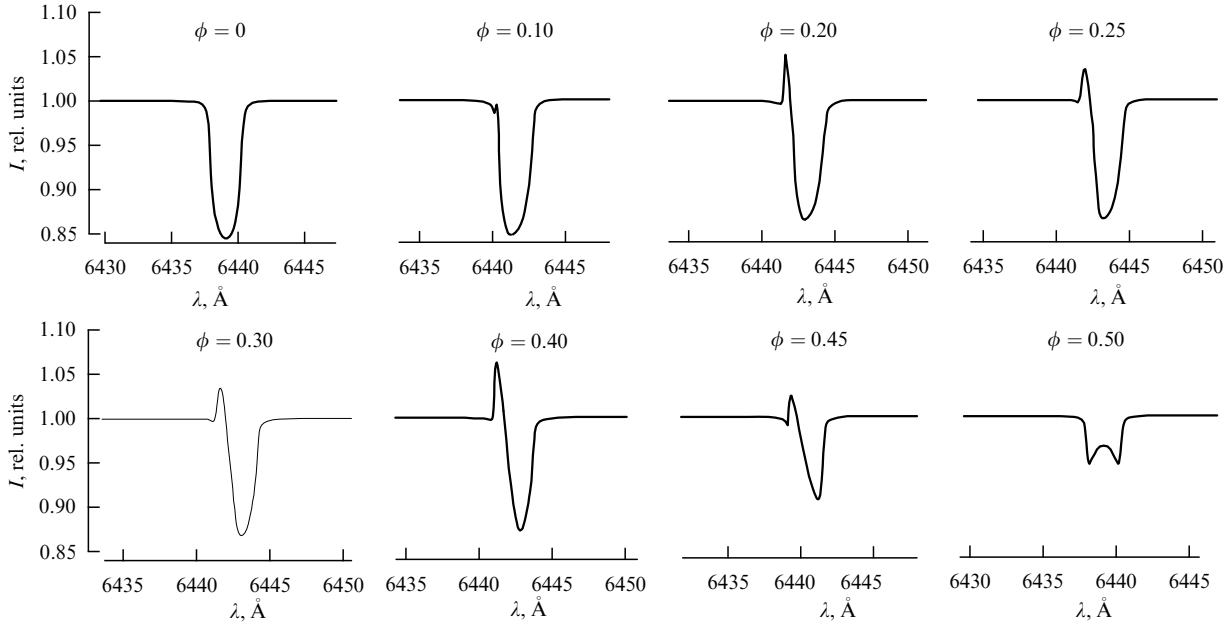

Figure 5. Change in the CaI, $\lambda = 6439$ Å, line profile in the spectrum of a low-mass binary with the orbital phase ϕ. It is assumed that $q = M_{BH}/M_v = 5$, the X-ray heating coefficient is $k_X = 10$, the binary inclination angle is $i = 90°$. (From paper [32].)

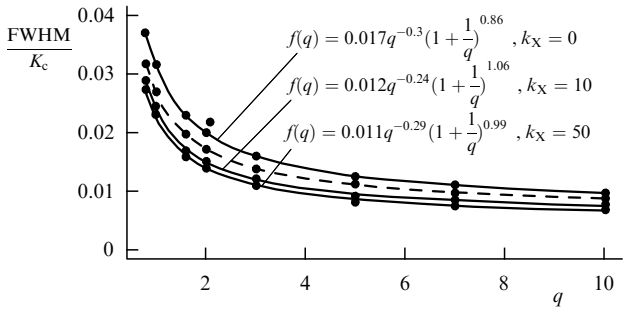

Figure 6. Values of $f(q) = \mathrm{FWHM}/K_c$ as a function of the mass ratio $q = M_{BH}/M_v$. Here, FWHM is the semi-width of the absorption line in the optical companion spectrum. Calculations are done for the model of a real tidally distorted star for different X-ray heating coefficients: $k_X = 0$, 10, 50. The orbital phase is $\phi = 0.25$. The dashed curve shows the result for a spherical star with the equivalent Roche-lobe volume with a constant local disk profile across the disk. (From [32].)

location on the stellar surface. The question arises as to how strong the approximations described above (flat circle, constant local profile, linear limb darkening law) alter the value of $v_{rot} \sin i$ and how this affects the mass ratio q derived from formula (3).

In [32], this question is studied in detail and it is concluded that these simplifying assumptions underestimate the value of q compared to the realistic model (Fig. 6). This underestimation is especially acute for large q (which is typical for BH LMXBs), up to several dozen percent. This has only a minor effect on the BH mass [see Eqn (1)], but the underestimation of q significantly affects the optical star mass:

$$M_v = \frac{M_{BH}}{q}\,.$$

To improve the mass ratio q, the values of q obtained in many papers should be increased (see, e.g., [40]), in agreement with Fig. 6. Then the improved optical star mass significantly decreases.

For example, for the BH LMXB X-ray nova V404 Cyg, the approximate values are $q = 16$, $M_{BH} = 8.4\,M_\odot$, and $M_v = 0.53\,M_\odot$ [40], and the improved values are $q = 23$, $M_{BH} = 8.4\,M_\odot$, and $M_v = 0.36\,M_\odot$ [32]. Here, we assume that $i = 67^\circ$ [42].

Thus, a more accurate analysis of the spectra of optical companions in BH LMXBs results in a significant decrease (by about 1.5 times) in the optical star masses, which aggravates difficulties in theoretical evolutionary scenarios of BH LMXBs with common envelopes.

One of the possible ways to overcome these difficulties might be related to accounting for a significant stellar wind mass loss from the optical star in BH LMXBs due to strong X-ray heating from an accreting BH [43–45]. It can be assumed that during the common envelope stage, the low-mass companion had a sufficiently high initial mass (more than $M_\odot$) in order to expel the common envelope. However, during the subsequent mass exchange with the accretion disk formation around the BH, the mass of the optical companion significantly decreased, mainly due to its intensive 'evaporation' by a powerful X-ray flux from the accreting BH (according to [44, 45], the mass loss by stellar wind from the companion induced by X-ray heating is an order of magnitude higher than the mass transfer rate onto the BH through the inner Lagrange point). The powerful stellar wind from the companion induced by the strong X-ray heating can form a circumbinary shell, whose interaction with the LMXB should result in a noticeable secular shortening of the LMXB orbital period. Such a shortening of the orbital period was recently discovered in two BH LMXBs [46]: XTEJ1118+480 ($\dot{P} = -1.90 \pm 0.57$ ms yr^{-1}) and A0620-00 ($\dot{P} = -0.60 \pm 0.08$ ms yr^{-1}). The significant mass loss from the optical companion can result in an excess of its effective temperature over that of ordinary low-mass stars [25]. Therefore, the initial mass of the optical companion should not be much greater that $M_\odot$.

Other interesting aspects of stellar-mass BHs are discussed in reviews [13, 17]. Here, we just present a short list of the latest important results related to stellar-mass BHs.

Using optical spectroscopy, Fabrika et al [47] showed that most of the ultraluminous X-ray sources (ULX) in other galaxies, which shine in X-rays a thousand times as strong as BHs in our Galaxy, can be supercritical accretion disks in close binaries with BHs, like the supercritically accreting microquasar SS433 in our Galaxy [48]. This conclusion is supported by detailed Doppler spectroscopic optical observations of some ULXs. For example, ULX P13 in NGC7793 is shown [49] to be a binary system with an orbital period of about 64 days. The mass-donating star in this system is a B9Ia supergiant illuminated by powerful X-ray emission from an accreting BH with a mass below $15\,M_\odot$. The authors of [49] conclude that the soft X-ray spectrum of this object suggests supercritical accretion onto a stellar-mass BH in this system. An intermediate-mass BH ($M_{BH} \simeq 10^3\,M_\odot$) in this system has not been discovered. According to [50], the mass-donating star in ULX J004722-252051 in NGC253 is a red supergiant around a BH with a mass of several dozen solar masses. ULX X-2 in M82 was discovered to be an X-ray pulsar [51]. A strongly magnetized neutron star was shown to be the source of the powerful X-ray emission in this system.

The ULX in the blue compact dwarf galaxy UGC6456 (VIIZw403) was discovered as a transient X-ray source [52].

In [53], quasiperiodic X-ray oscillations with the quasi-period ratio 3:2 were discovered from the ULX X-1 in the galaxy M82 and the mass of the accreting BH was estimated to be $400\,M_\odot$.

The discovery of baryonic jets from an assumed BH in the X-ray binary system 4U1630-70 is reported in [54]; this can be an analog of SS433 [48].

Quasi-synchronous X-ray (Chandra space X-ray telescope) and optical (Hubble Space Telescope) observations of the BH X-ray binary NGC300X-1 with a WR star were carried out in [55]. It is noted that the error box of the source X-1 contains both the WR star and a comparatively low-mass AGB (asymptotic giant branch) star. Therefore, it has not been ruled out that the system NGC300X-1 is not a WR + BH system but an AGB + BH system. The WR + BH model in [55] suggests that the X-ray eclipse minimum corresponds to the radial velocity maximum as measured from the HeII4686 emission line. Hence, this line should not reflect the orbital motion of the components. Therefore, the BH mass estimate in the WR + BH model ($M_{BH} = 17 \pm 6\,M_\odot$) obtained earlier [56] can be uncertain. In another X-ray binary system, WR + BH IC10X-1, the radial velocity curve calculated from the HeII4686 emission line was inspected to correspond to the X-ray eclipse minimum. In this system, located in the galaxy IC10, as in the system NGC300X-1, the middle of the X-ray eclipse also corresponds to the radial velocity curve

maximum calculated from the HeII4686 emission line, suggesting that the radial velocity curve inferred from this emission line apparently does not reflect the orbital motion of the WR star, and therefore the BH mass estimate obtained in [58] ($M_{\rm BH} = (28 \pm 5)\, M_\odot$) is uncertain. This possibility in the systems NGC300X-1 and IC10X-1 was mentioned in our book [18].

Presently, the optical companions in 184 X-ray binary systems are known to be rapidly rotating Be-stars [59]. The majority of these systems have neutron stars as the accreting companions. The discovery of a BH ($M_{\rm BH} \simeq 5\, M_\odot$) paired with a Be-star ($M_{\rm Be} \simeq 13\, M_\odot$) is reported in [60] (the X-ray binary system in the galaxy MWC656 with an orbital period of about 60 days). The presence of a BH in a Be X-ray binary poses new questions in the binary star evolution theory. The end stage of evolution of such Be + BH binaries should be the coalescence of the BH with the neutron star, which should lead to a powerful burst of gravitational waves [60]. The detection rate of such coalescences by the advanced LIGO/Virgo interferometers can be as high as one event every five years [60].

A stationary compact radio counterpart of the X-ray source X9 was discovered in the massive ($M = 6.5 \times 10^5\, M_\odot$) globular cluster 47Tuc [61], suggesting the presence of a low-mass X-ray binary system with a BH.

Anomalies in the chemical composition in the optical spectrum were used in [62] to find the first reliable candidate for a Thorne–Zytkow object [63] — a neutron star in the center of a fully convective red giant.

In [64], the estimated angular momenta of BHs in LMXBs are interpreted in terms of the spin-up of BHs accreting from low-mass stars ($M \simeq (1-2)\, M_\odot$). It is shown that the observed angular momenta of stellar-mass BHs can be easily explained by the storage of angular momentum of the accreting matter transferred from the optical star. It is also shown that the observed BH masses in LMXBs are on average by $1.3\, M_\odot$ larger (because of the accreted mass) than their initial masses.

We also note the recent data on X-ray novae with BHs, which are also BH LMXBs. In 2015, after a 25-year 'silence', the X-ray nova V404 Cyg demonstrated a powerful outburst [65, 66]. This BH LMXB has shown several outbursts, at least three having been registered: in 1938, 1956 (recorded in the archive of photographic optical observations), and 1989 (detected by X-ray space observatories [67] and by ground-based photoelectric observations [68]). The 2015 outburst of V404Cyg turned out to be very unusual: the X-ray and optical light curves demonstrate a fast chaotic variability [66]. The 2015 outburst of V404Cyg differs greatly from the 1938 and 1989 outbursts. Because the X-ray nova outbursts are due to instabilities in the accretion disk, the results of the 2015 observations are important for the theory of nonstationary disk accretion onto BHs.

Quasi-synchronous X-ray and optical observations of the X-ray nova with BH MAXIJ1828-249 are reported in [69]. It is shown that the optical and infrared emission from this X-ray nova are largely determined by a continuation of the power-law spectral component that is responsible for its hard X-ray emission The contribution from cold outer parts of the accretion disk, even with the X-ray heating taken into account, is moderate during the 'high' state of the system (when a soft black-body component dominates in the X-ray spectrum) and is virtually absent during the 'low' ('hard') state.

3. Supermassive black holes in active galactic nuclei

Using the most reliable tools (the method of resolved kinematics, including dynamics of stars, gas and maser sources [70], and the reverberation method [71–74]), high-quality measurements of several hundred SMBHs in active galactic nuclei have been carried out.

We note that the first estimates of SMBH masses in active galactic nuclei — quasars — were obtained in 1964 in the pioneering paper by Zel'dovich and Novikov [75] under the reasonable assumption that the luminosities of quasars — accreting BHs — are close to the critical Eddington luminosity.

The most reliable central BH masses in 44 elliptical galaxies and 41 spiral galaxies, mainly determined by the resolved kinematics method from Hubble Space Telescope observations, are reported in the superb review by Kormendy and Ho [70]. These masses range from $(0.94-1.34) \times 10^6\, M_\odot$ to $(0.49-3.66) \times 10^{10} M_\odot$ (the intervals in the parentheses characterize the mass determination error). Reliable determinations of the masses of SMBHs and of central star clusters for 82 galaxies with known rotational velocities (i.e., with known total masses, including the mass of the dark matter halo) are summarized in [76]. The authors of [77] use the Sloan Digital Sky Survey (SDSS) data corrected for incompleteness to construct the SMBH mass function for 9886 quasars as a function of the redshift z in the range $1 < z < 4.5$. The BH masses were determined by an express method based on the observed quasar luminosities, as well as using the widths and intensities of emission lines in their spectra. The SMBH mass function found in such a way (with observational selection effects taken into account) turns out to be shifted toward higher masses with the increase in the redshift z (the decrease in the proper age of a quasar). It is concluded in [78] that the mass of the central SMBH increases with the redshift relative to the galactic bulge mass. The discovery of more than a dozen quasars with a redshift $z > 6$ (the proper age of the quasar being less than one billion years) and with high central BH masses ($M_{\rm BH} \simeq (10^8 - 10^9)\, M_\odot$) suggests that the formation time of SMBHs is relatively short, less than a billion years. For example, in [79], the SMBH mass in a quasar with a very high redshift $z = 7.085$ is reported: the proper age of the quasar is 770 mln years, which turns out to be very large: $M_{\rm BH} \simeq (2.0^{+1.5}_{-0.7}) \times 10^9\, M_\odot$.

Thus, an astonishing fact arises: the younger an SMBH is, the higher on average its mass, and the formation time of the most massive and comparatively young BHs (at large redshifts) is relatively short: less than a billion years, with the age of the Universe being ~ 14 bln years. This important observational fact, unless contaminated by observational selection effects, requires a special theoretical investigation. Possibly, the growth of mass in the central SMBH is additionally stimulated by galaxy mergers, which occur especially intensively at early stages of the evolution of the Universe ($z = 1-5$). To explain the shift of the SMBH mass function toward higher masses with the redshift found in [77], the authors of [80] used a model of SMBH mass growth based on a hierarchical structure formation, according to which the growth of an SMBH is due to a merging of BHs with smaller masses and accretion of the ambient gas at a rate limited by the Eddington luminosity. It is shown in [80] that the evolution in the model with a low-mass BH seed (the BH remnant of a population-III star with a mass of several

hundred $M_\odot$) does not enable the observed SMBH mass function for $M_{BH} > 10^9\,M_\odot$ in the range $1 < z < 4.5$. At the same time, the model with massive seeds ($M_{BH} = (10^5-10^6)\,M_\odot$) (e.g., BHs formed from the collapse of a pre-galactic hydrogen–helium disk) enables the observed SMBH mass function for $M_{BH} > 10^9\,M_\odot$ at $z > 2$, and is therefore favorable.

In recent years, the important role of both SMBHs and massive-star clusters in the centers of galaxies has become clear [76, 81–83]. It is argued that SMBHs exist in galaxies with massive spherical stellar components (for example, in massive elliptical galaxies or early-type spirals with massive bulges, $M_{sph} > 10^{10}\,M_\odot$). However, in most galaxies without massive stellar spheroids, SMBHs are found quite rarely [84]. In galaxies with intermediate-mass spheroids ($10^8\,M_\odot \lesssim M_{sph} \lesssim 10^{10}\,M_\odot$), there are both SMBHs and massive star clusters with comparable masses [85]. An important correlation between the SMBH masses, the masses of central star clusters, and the parameters of spheroid components of galaxies arises:

$$M \sim \sigma^\beta,$$

where M is the mass of the SMBH or central star cluster and σ is the velocity dispersion of the spheroid component. The power-law exponent is $\beta = 4-5$ for SMBHs (see, e.g., [86]), and β lies in the range from 1.57 ± 0.24 [86] to 2.73 ± 0.29 [84] for central massive-star clusters. Thus, the dependence of the central star cluster masses on the velocity dispersion σ is weaker ($\beta = 1.57-2.73$) than for central SMBHs ($\beta = 4-5$). This suggests a different formation and evolution of the central SMBHs and massive star clusters in galactic nuclei.

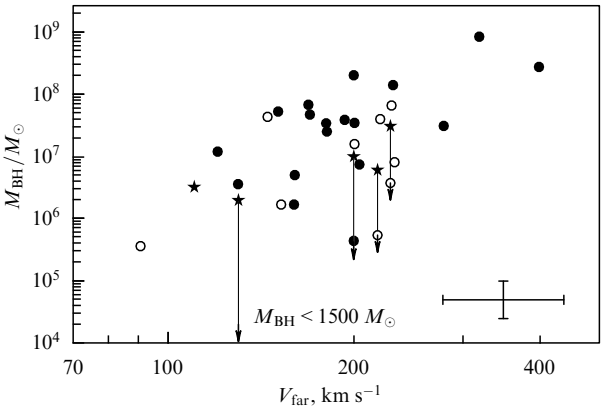

Figure 7. Limiting rotational velocity of a galaxy, V_{far}, as a function of the central SMBH mass (from paper [81]). The filled and open circles mark black holes and star clusters, respectively. The filled stars correspond to central massive star clusters. The arrows are for the upper mass limits.

In recent review [70], these general considerations of the formation and evolution of SMBHs were further developed using the latest observational data. It is shown that the parameters of SMBHs correlate differently with different galactic components. The SMBH masses closely correlate only with parameters of classical bulges and elliptical galaxies. At the same time, the SMBH masses very weakly correlate with parameters of pseudo-bulges and galactic haloes, which mainly consist of dark matter. In addition, SMBHs show no correlation at all with the parameters of galactic disks. We recall that the bulge is the central spherical part of a galaxy, which consists of old low-mass stars with large velocity dispersion, and the pseudo-bulge is a thickening in the central part of a galaxy with enhanced velocity dispersion of stars (the 'heated' part of the stellar population of the galactic disk).

Our studies of galactic rotational velocities with known SMBH masses [76, 81, 87, 88] are in general agreement with the conclusions in review [70], the only difference being that according to our data, there is a relation, albeit very indirect, between the central SMBHs and dark matter in galaxies.

Figure 7 shows the limit rotational velocity of a galaxy as a function of the central SMBH mass [81]. This dependence is rather loose, suggesting an indirect relation, if any, between galactic dark matter and the central SMBH mass, in agreement with the conclusions in [70]. However, a more sophisticated analysis reveals that such a relation is still significant for galaxies. In Fig. 8, taken from [81], plots of two dependences are presented: between the central SMBH mass and the galactic optical luminosity (baryonic matter), which are virtually uncorrelated, and between the central SMBH masses for the same galaxy sample and the indicative galactic masses, $M_{25} = V_{far}^2 R_{25}/G$, which are clearly correlated. Here, R_{25} is the radius corresponding to the galactic surface brightness of the 25th magnitude from a square arcsec. This radius defines the visible boundary of a galaxy.

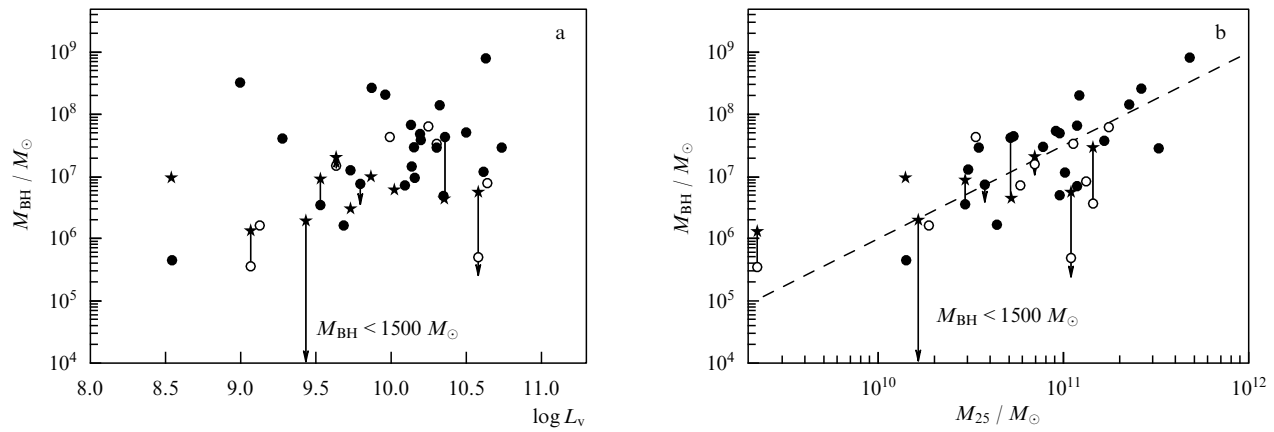

Figure 8. Comparison of masses of supermassive black holes (a) with the total optical luminosity of the host galaxy, L_v, characterizing baryonic matter, and (b) with the indicative galactic mass (for the same galaxies), $M_{25} = V_{far}^2 R_{25}/G$, including both baryonic and dark matter. The black stars correspond to central star clusters. The line segments join circles (black holes) and stars (clusters), corresponding to one galaxy. The arrows indicate the upper mass limits. (From paper [81].)

The indicative mass includes both the baryonic mass and dark matter, which dominates. It follows from Fig. 8 that the addition of dark matter to the baryonic mass significantly strengthens the correlation. This suggests that the role of dark matter in the formation of a central SMBH, although indirect (see Fig. 7), is still significant (see Fig. 8).

In the work of Gurevich's group [89], it is shown that gravitational instability in protogalactic dark matter clumps gives rise to deep and sharp potential minima (cusps), into which the baryonic matter 'falls' to form the stellar population of a forming galaxy. This process can stimulate the central SMBH formation. Therefore, a relation between the central SMBH mass and the galactic dark matter halo mass might exist. However, due to galaxy mergers at early stages, as well as star formation in galactic centers, this relation can be very indirect, which is indeed observed (see Fig. 7). The relation between the SMBH mass and the virial mass of a galaxy is predicted in numerical cosmological simulations [89–92].

An approximate formula relating the central SMBH mass and the galactic bulge mass $M_{\rm bulge}$ is given in [70]. This formula is based on the most reliable observational data (pseudobulges, for which the correlation is poor, as well as merging galaxies, etc., are ignored):

$$\frac{M_{\rm BH}}{10^9 M_\odot} = (0.49^{+0.06}_{-0.05})\left(\frac{M_{\rm bulge}}{10^{11} M_\odot}\right)^{1.17\pm0.08}.$$

It follows that for the bulge mass $M_{\rm bulge} = 10^{11} M_\odot$, the relation between the central SMBH mass and the bulge is

$$\frac{M_{\rm BH}}{M_{\rm bulge}} = 0.49^{+0.06}_{-0.05}\%\,,$$

i.e., for a $10^{11} M_\odot$ bulge, about 0.5% of its mass is in the central SMBH. An improved approximate formula relating the central SMBH mass to the stellar velocity dispersion σ in the bulge is also presented in [70]:

$$\frac{M_{\rm BH}}{10^9 M_\odot} = 0.310^{+0.037}_{-0.033}\left(\frac{\sigma}{200\ {\rm km\ s^{-1}}}\right)^{4.38\pm0.29}. \qquad (4)$$

Various aspects of the coevolution of SMBHs and host galaxies are discussed in [70]. The coevolution means mutual evolutionary effects between the SMBH and the host galaxy. Weak coevolution assumes an influence of the galaxy on the SMBH via accretion of galactic gas and stars onto the SMBH, galaxy mergers, etc. Strong coevolution occurs, for example, in active galactic nuclei and quasars, where huge accretion rates close to the Eddington limit give rise to the formation of powerful matter outflows from supercritical accretion disks around the central SMBHs (powerful winds, relativistic jets, etc.). This leads to the sweeping out of gas from the host galaxy, cessation of the SMBH mass growth, and star formation quenching in the host galaxy.

It is shown in [76] that the strong coevolution of the central SMBH and the host galaxy may cause large color indexes ($B-V>0.6-0.7$) of the 'red' group g-type galaxies with weak star formation. The 'red' galaxies significantly differ from blue galaxies, which have higher masses of SMBHs and central star clusters.

We now turn to crucial experiments with high angular resolution (better than 10^{-5} arcsec). Results of observations of radio jets from SMBHs in galactic nuclei with the high angular resolution better than 10^{-5} arcsec by the Radio-astron space radio interferometer were presented by N S Kardashev at the Scientific Session of the Physical Sciences Division Russian Academy of Sciences, on December 23, 2015. In particular, observations of BL Lacertae (BL Lac) with a record high angular resolution of 21 micro arcsec is reported in [93]. Kardashev also reported on the prospects of probing the vicinity of SMBH event horizons in galactic nuclei by the Millimetron planned space interferometer with a huge angular resolution, up to 10^{-8} arcsec.

In recent years, a ground-based VLBI interferometer at short waves ($\lambda \lesssim 1.3$ mm), the EHT (Event Horizon Telescope), has been under construction, which aims at imaging a 'shadow' from the central Galactic SMBH, as well as from the SMBH in the nearby galaxy M87 [10, 94]. The EHT consists of a global network of sub-mm radio dishes located in the USA, Germany, Japan, Chile, and Taiwan. The angular resolution of the EHT will be 23 marcsec at a frequency of 230 GHz ($\lambda \approx 1.3$ mm) and 15 marcsec at 345 GHz ($\lambda \approx 0.9$ mm) [94]. The first results of observations of SMBHs in our Galaxy center and the M87 galaxy, obtained with a limited number of radio telescopes, have already been published [7–9]. At wavelengths shorter than 1.3 mm, the radio emission scattering on the interstellar plasma inhomogeneities is insignificant for the SMBH in our Galaxy center and in M87; therefore, in this case, it is possible to observe a 'shadow' from the SMBH on the accretion disk and relativistic jet emission. In the case of a Schwarzschild BH, the linear size $d_{\rm sh}$ of the shadow is approximately 2.6 times the double Schwarzschild BH radius due to the complex distortion of photon trajectories near the BH event horizon (photons move along circular trajectories [95]): $d_{\rm sh} = 2\sqrt{27}\,GM/c^2$ (see, e.g., [94]). For the Galactic SMBH ($M_{\rm BH} = 4.31\times10^6 M_\odot$) at the distance $D = 8.33$ kpc, the angular diameter of the 'shadow' is $d_{\rm sh} = 5.3\times10^{-5}$ arcsec; for the SMBH in M87 (with $M_{\rm BH} = 6.6\times10^9 M_\odot$ and $D = 1.79\times10^4$ kpc), $d_{\rm sh} = 3.78\times10^{-5}$ arcsec [94].

Thus, the EHT will be able to 'see' images of 'shadows' from SMBHs in the center of our Galaxy and in M87. Hopefully, this challenging and extremely important problem will be solved in the nearest future. Recently, the first results of EHT observations of linear polarization of radio emission and the structure of the regular magnetic field on a scale of about six Schwarzschild radii from the event horizon of the SMBH in our Galaxy center were reported [10]. The authors of [10], in addition, discovered the variability of the magnetic field structure in this region on time scales shorter than one hour. The authors of [10] conclude that the optimal (according to the χ^2 test) model of a Gaussian circular brightness distribution (with no central brightness decrease) with the FWHM equal to 5.2×10^{-5} arcsec is definitely refuted by the EHT observations. Of the models consistent with the EHT observations, the simplest model represents a bright ring of constant intensity (the inner and outer ring diameters are 2.1×10^{-5} and 9.7×10^{-5} arcsec). Thus, preliminary (in the opinion of the authors of [10]) observations of the brightness distribution in the vicinity of the Galactic central SMBH do not contradict the model with a central dark 'shadow'. The authors of [10] argue that further VLBI observations by the EHT including additional sub-mm radio dishes will not only improve the magnetic field distribution and their variability in the Galaxy center but also provide a more reliable imaging of the Galactic SMBH 'shadow' region, which is necessary to check the applicability of General Relativity in extremely strong gravitational fields.

General Relativity tests in strong gravitational fields that can be performed by observations of the central Galactic SMBH are summarized in [96] (see also [94, 97]). These tests include measurements of the relativistic shift of the pericenter of stellar orbits around the SMBH; the precise timing of radio pulsars orbiting an SMBH that is sensitive to the SMBH spin and to its possible quadruple moment; VLBI observations by the EHT of the SMBH 'shadow', whose size and shape are sensitive to the generalized Kerr metric as well as to various extensions of GR.

Recently, a new aspect of SMBH observations in galactic nuclei emerged: the study of binary SMBHs (see, e.g., [98–100]). Binary SMBHs could be formed in the hierarchical galaxy formation model during galaxy mergings (see, e.g., [101–103]).

Supermassive objects in galactic centers could also be wormholes [11]. The search for wormholes — tunnels in space–time — is included in the scientific program of the Radioastron and Millimetron space interferometers (see also the paper by Novikov [104]).

To conclude, we note the recent paper [105], which presents an important observational argument favoring the presence of an event horizon in the central SMBH in M87. This SMBH produces a powerful extended relativistic collimated jet. In addition, VLBI observations by the EHT enabled localizing the emission from the jet base on an angular scale comparable to the SMBH event horizon [9]. The authors of [105] note that, irrespective of the jet formation mechanism, its observed power should be provided by a certain minimum mass accretion rate onto the SMBH. If the compact object in the M87 center is not a BH and has an observable surface, the accretion should lead to a significant energy release on this surface in the near-infrared and optical spectral ranges. Estimates of the upper limits of the infrared and optical fluxes from the M87 center made in [105] turn out to be at least an order of magnitude below the fluxes that would be expected from the M87 central compact object with a surface, disproving the hypothesis of a central object with a surface and indirectly supporting the presence of the event horizon in the central object in M87.

4. Conclusion

We presented recent observational studies of extreme objects in the Universe: black holes.

With the gravitational waves having been discovered [6], we can hope that modern gravitational wave antennas with improved sensitivity will allow 'hearing the bell' of many coalescing binary stellar mass black holes, and ground-based and space interferometers (EHT, Millimetron) will provide imaging of SMBHs in galactic nuclei. This will give strong impetus to the development of the extremely interesting physics and astrophysics of black holes.

References

1. Zel'dovich Ya B *Sov. Phys. Dokl.* **9** 195 (1964); *Dokl. Akad. Nauk SSSR* **155** 67 (1964)
2. Salpeter E E *Astrophys. J.* **140** 796 (1964)
3. Shakura N I, Sunyaev R A *Astron. Astrophys.* **24** 337 (1973)
4. Pringle J E, Rees M J *Astron. Astrophys.* **21** 1 (1972)
5. Novikov I D, Thorne K S, in *Black Holes* (Eds C DeWitt, B S DeWitt) (New York: Gordon and Breach, 1973) p. 343
6. Abbott B P et al. (LIGO Sci. Collab., Virgo Collab.) *Phys. Rev. Lett.* **116** 061102 (2016)
7. Doeleman S S et al. *Nature* **455** 78 (2008)
8. Fish V L et al. *Astrophys. J.* **727** L36 (2011)
9. Doeleman S S et al. *Science* **338** 355 (2012)
10. Johnson M D et al. *Science* **350** 1242 (2015); arXiv:1512.01220
11. Kardashev N S et al. *Phys. Usp.* **57** 1199 (2014); *Usp. Fiz. Nauk* **184** 1319 (2014)
12. Gillessen S et al. *Astrophys. J.* **692** 1075 (2009)
13. Cherepashchuk A M *Phys. Usp.* **57** 359 (2014); *Usp. Fiz. Nauk* **184** 387 (2014)
14. Scheel M A, Thorne K S *Phys. Usp.* **57** 342 (2014); *Usp. Fiz. Nauk* **184** 367 (2014)
15. Lipunov V M, Postnov K A, Prokhorov M E *New Astron.* **2** 43 (1997)
16. Lipunov V M, Postnov K A, Prokhorov M E *Mon. Not. R. Astron. Soc.* **288** 245 (1997)
17. Casares J, Jonker P G *Space Sci. Rev.* **183** 223 (2014)
18. Cherepashchuk A M *Tesnye Dvoinye Zvezdy* (Close Binary Stars) Vol. 1 (Moscow: Fizmatlit, 2013); Cherepashchuk A M *Tesnye Dvoinye Zvezdy* (Close Binary Stars) Vol. 2 (Moscow: Fizmatlit, 2013)
19. Massevich A G, Tutukov A V *Evolyutsiya Zvezd: Teoriya i Nablyudeniya* (Evolution of Stars: Theory and Observations) (Moscow: Nauka, 1988)
20. Abubekerov M K, Antokhina E A, Bogomazov A I, Cherepashchuk A M *Astron. Rep.* **53** 232 (2009); *Astron. Zh.* **86** 260 (2009)
21. Portegis Zwart S F, Verbunt F, Ergma E *Astron. Astrophys.* **321** 207 (1997)
22. Kalogera V *Astrophys. J.* **521** 723 (1999)
23. Podsiadlowski P, Rappaport S, Han Z *Mon. Not. R. Astron. Soc.* **341** 385 (2003)
24. Kiel P D, Hurley J R *Mon. Not. R. Astron. Soc.* **369** 1152 (2006)
25. Wang C, Jia K, Li X-D *Mon. Not. R. Astron. Soc.* **457** 1015 (2016); arXiv:1601.02721
26. Israelian G et al. *Nature* **401** 142 (1999)
27. Brandt W N, Podsiadlowski Ph, Sigurdsson S *Mon. Not. R. Astron. Soc.* **277** L35 (1995)
28. Orosz J A et al. *Astrophys. J.* **555** 489 (2001)
29. Wagner R M et al. *Astrophys. J.* **556** 42 (2001)
30. Mirabel I F et al. *Nature* **413** 139 (2001)
31. Petrov V S, Antokhina E A, Cherepashchuk A M *Astron. Rep.* **57** 669 (2013); *Astron. Zh.* **90** 729 (2013)
32. Petrov V S, Antokhina E A, Cherepashchuk A M *Astron. Rep.* **59** 346 (2015); *Astron. Zh.* **92** 386 (2015)
33. Lyutyi V M, Syunyaev R A, Cherepashchuk A M *Sov. Astron.* **17** 1 (1973); *Astron. Zh.* **50** 3 (1973)
34. Lyutyi V M, Syunyaev R A, Cherepashchuk A M *Sov. Astron.* **18** 684 (1975); *Astron. Zh.* **51** 1150 (1974)
35. Wu J et al. *Astrophys. J.* **825** 46 (2016); arXiv:1601.00616
36. Wade R A, Horne K *Astrophys. J.* **324** 411 (1988)
37. Antokhina E A, Cherepashchuk A M *Astron. Rep.* **38** 367 (1994); *Astron. Zh.* **71** 420 (1994)
38. Antokhina E A *Astron. Rep.* **40** 483 (1996); *Astron. Zh.* **73** 532 (1996)
39. Antokhina E A, Cherepashchuk A M, Shimanskii V V *Astron. Rep.* **49** 109 (2005); *Astron. Zh.* **82** 131 (2005)
40. Casares J, Charles P A *Mon. Not. R. Astron. Soc.* **271** L5 (1994)
41. Collins G W (II), Truax R J *Astrophys. J.* **439** 860 (1995)
42. Khargharia J, Froning C S, Robinson E L *Astrophys. J.* **716** 1105 (2010)
43. Basko M M, Sunyaev R A, Titarchuk L G *Astron. Astrophys.* **31** 249 (1974)
44. Iben I (Jr.), Tutukov A V, Yungelson L R *Astrophys. J. Suppl.* **100** 217 (1995)
45. Iben I (Jr.), Tutukov A V, Yungelson L R *Astrophys J. Suppl.* **100** 233 (1995)
46. Gonzáles Hernández J I, Rebolo R, Casares J *Mon. Not. R. Astron. Soc.* **438** L21 (2014)
47. Fabrika S et al. *Nature Phys.* **11** 551 (2015)
48. Cherepashchuk A M *Mon. Not. R. Astron. Soc.* **194** 761 (1981)
49. Motch C et al. *Nature* **514** 198 (2014); arXiv:1410.4250
50. Heida M et al. *Mon. Not. R. Astron. Soc.* **453** 3510 (2015)
51. Bachetti M et al. *Nature* **514** 202 (2014)
52. Brorby M, Kaaret P, Feng H *Mon. Not. R. Astron. Soc.* **448** 3374 (2015)

53. Pasham D R, Strohmayer T E, Mushotzky R F *Nature* **513** 74 (2014)
54. Díaz Trigo M et al. *Nature* **504** 260 (2013)
55. Binder B et al. *Mon. Not. R. Astron. Soc.* **451** 4471 (2015)
56. Crowther P A et al. *Mon. Not. R. Astron. Soc.* **403** L41 (2010)
57. Laycock S G T, Cappallo R C, Moro M J *Mon. Not. R. Astron. Soc.* **446** 1399 (2015)
58. Prestwich A H et al. *Astrophys. J.* **669** L21 (2007)
59. Ziolkowski J *Acta Polytech. CTU Proc.* **1** (1) 175 (2014); in *Proc. of the 10th Intern. Workshop on Multifrequency Behaviour of High Energy Cosmic Sources, Palermo, Italy, 2013*
60. Casares J et al. *Nature* **505** 378 (2014)
61. Miller-Jones J C A et al. *Mon. Not. R. Astron. Soc.* **453** 3918 (2015)
62. Levesque E M et al. *Mon. Not. R. Astron. Soc.* **443** L94 (2014); arXiv:1406.0001
63. Thorne K S, Zytkow A N *Astrophys. J.* **212** 832 (1977)
64. Fragos T, McClintock J E *Astrophys. J.* **800** 17 (2015)
65. Kuulkers E et al., Astronomer's Telegram. ATel (7647) (2015)
66. Bernardini F et al. *Astrophys. J.* **818** L5 (2016)
67. Syunyaev R A et al. *Sov. Astron. Lett.* **17** 123 (1991); *Pis'ma Astron. Zh.* **17** 291 (1991)
68. Goranskii V P et al. *Astron. Lett.* **22** 371 (1996); *Pis'ma Astron. Zh.* **22** 413 (1996)
69. Grebenev S A et al. *Astron. Lett.* **42** 69 (2016); *Pis'ma Astron. Zh.* **42** 88 (2016)
70. Kormendy J, Ho L C *Annu. Rev. Astron. Astrophys.* **51** 511 (2013)
71. Cherepashchuk A M, Lyutyi V M *Astrophys. Lett.* **13** 165 (1973)
72. Antokhin I I, Bochkarev N G *Sov. Astron.* **27** 261 (1983); *Astron. Zh.* **60** 448 (1983)
73. Blandford R D, McKee C F *Astrophys. J.* **255** 419 (1982)
74. Gaskell C M, Sparke L S *Astrophys. J.* **305** 175 (1986)
75. Zel'dovich Ya B, Novikov I D *Sov. Phys. Dokl.* **9** 834 (1965); *Dokl. Akad. Nauk SSSR* **158** 811 (1964)
76. Zasov A V, Cherepashchuk A M *Astron. Rep.* **57** 797 (2013); *Astron. Zh.* **90** 871 (2013)
77. Kelly B C et al. *Astrophys. J.* **719** 1315 (2010)
78. Decarli R et al. *Mon. Not. R. Astron. Soc.* **402** 2453 (2010)
79. Mortlock D J et al. *Nature* **474** 616 (2011)
80. Natarajan P, Volonteri M *Mon. Not. R. Astron. Soc.* **422** 2051 (2012)
81. Zasov A V, Cherepashchuk A M, Katkov I Yu *Astron. Rep.* **55** 595 (2011); *Astron. Zh.* **88** 648 (2011)
82. Ferrarese L et al. *Astrophys. J.* **644** L21 (2006)
83. Wehner E H, Harris W E *Astrophys. J.* **644** L17 (2006)
84. Leigh N, Böker T, Knigge C *Mon. Not. R. Astron. Soc.* **424** 2130 (2012)
85. Graham A W, Spitler L R *Mon. Not. R. Astron. Soc.* **397** 2148 (2009)
86. Graham A W *Mon. Not. R. Astron. Soc.* **422** 1586 (2012)
87. Cherepashchuk A M et al. *Astron. Rep.* **54** 578 (2010); *Astron. Zh.* **87** 634 (2010)
88. Zasov A V, Petrochenko L N, Cherepashchuk A M *Astron. Rep.* **49** 362 (2005); *Astron. Zh.* **82** 407 (2005)
89. Ilyin A S, Zybin K P, Gurevich A V *JETP* **98** 1 (2004); *Zh. Eksp. Teor. Fiz.* **125** 5 (2004)
90. Ferrarese L *Astrophys. J.* **578** 90 (2002)
91. Di Matteo T et al. *Astrophys. J.* **593** 56 (2003)
92. Booth C M, Schaye J *Mon. Not. R. Astron. Soc.* **405** L1 (2010)
93. Gómez J L et al. *Astrophys. J.* **817** 96 (2016); arXiv:1512.04690
94. Ricarte A, Dexter J *Mon. Not. R. Astron. Soc.* **446** 1973 (2015)
95. Zakharov A F et al. *New Astron.* **10** 479 (2005)
96. Johannsen T *Class. Quantum Grav.* **33** 113001 (2016); arXiv:1512.03818
97. Angélil R, Saha P *Mon. Not. R. Astron. Soc.* **444** 3780 (2014)
98. Graham M J et al. *Nature* **518** 74 (2015)
99. Graham M J et al. *Mon. Not. R. Astron. Soc.* **453** 1562 (2015)
100. D'Orazio D J et al. *Mon. Not. R. Astron. Soc.* **452** 2540 (2015)
101. Haehnelt M G, Kauffmann G *Mon. Not. R. Astron. Soc.* **336** L61 (2002)
102. Volonteri M, Madau P, Haardt F *Astrophys. J.* **593** 661 (2003)
103. Colpi M *Space Sci. Rev.* **183** 189 (2014)
104. Novikov I D *Phys. Usp.* **59** 713 (2016); *Usp. Fiz. Nauk* **186** 790 (2016)
105. Broderick A E et al. *Astrophys. J.* **805** 179 (2015); arXiv:1503.03873